

## Pair Density Wave Order from Electron Repulsion

Yi-Ming Wu,<sup>1</sup> P. A. Nosov,<sup>1</sup> Aavishkar A. Patel,<sup>2</sup> and S. Raghu<sup>1</sup>

<sup>1</sup>Stanford Institute for Theoretical Physics, Stanford University, Stanford, California 94305, USA

<sup>2</sup>Center for Computational Quantum Physics, Flatiron Institute, New York, New York 10010, USA



(Received 30 September 2022; accepted 22 December 2022; published 13 January 2023)

A pair density wave (PDW) is a superconductor whose order parameter is a periodic function of space, without an accompanying spatially uniform component. Since PDWs are not the outcome of a weak-coupling instability of a Fermi liquid, a generic pairing mechanism for PDW order has remained elusive. We describe and solve models having robust PDW phases. To access the intermediate coupling limit, we invoke large- $N$  limits of Fermi liquids with repulsive BCS interactions that admit saddle point solutions. We show that the requirements for long-range PDW order are that the repulsive BCS couplings must be nonmonotonic in space and that their strength must exceed a threshold value. We obtain a phase diagram with both finite temperature transitions to PDW order and a  $T = 0$  quantum critical point, where non-Fermi liquid behavior occurs.

DOI: 10.1103/PhysRevLett.130.026001

**Introduction.**—A pair density wave (PDW) is a rare and exotic superconductor in which pairs of electrons condense with nonzero center of mass momentum [1]. Similar phases of matter were conceived decades ago by Fulde, Ferrel, Larkin, and Ovchinnikov (FFLO), in the context of spin-polarized superconductivity [2–7]. In addition to exhibiting the usual properties of superconductors, PDWs break translation symmetry and are therefore accompanied by charge modulation. PDW order is believed to occur in a variety of correlated electron materials [8–18], in cold atom systems [19–21]. More recently, they have been observed in the iron based superconductor  $\text{EuRbFe}_4\text{As}_4$  [22], the heavy fermion superconductor  $\text{UTe}_2$  [23], as well as the kagome metal  $\text{CsV}_3\text{Sb}_5$  [24]. In the absence of fine-tuning (e.g., perfectly nested Fermi surfaces in the particle-particle channel [25–30]), PDWs do not stem from a weak-coupling instability of a Fermi liquid, and robust mechanisms of PDW formation have therefore remained elusive, despite intense efforts [14,31–41].

It is easy to see why PDW order requires intermediate coupling. In a clean Fermi liquid with inversion and/or time-reversal symmetry, the static pair susceptibility is a positive-definite quantity that diverges logarithmically only at zero center of mass momentum  $\mathbf{q} = 0$ , reflecting the celebrated BCS instability. Away from  $\mathbf{q} = 0$ , the logarithmic divergence is cut off, and pairing with  $\mathbf{q} \neq 0$  requires a finite interaction strength. Therefore, many proposed mechanisms for FFLO superconductivity have relied on shifting the large pair susceptibility away from  $\mathbf{q} = 0$ , say by the application of a Zeeman field [2,3], or, say, by considering the effects of Rashba spin-orbit effects on odd parity superconductivity [42]. By contrast, we wish to ask whether there can be an *intrinsic* mechanism for

PDW order, which requires only the existence of sizable interactions.

In this Letter, we study various models of Fermi liquids in the presence of repulsive BCS interactions. We solve such theories beyond the weak-coupling regime by appealing to a large- $N$  limit whose saddle point corresponds to a self-consistent set of solutions for the propagators of the theory. From these solutions, we deduce the existence of both finite temperature continuous transitions to PDW order as well as a quantum critical point (QCP) at  $T = 0$  separating a Fermi liquid metal from a PDW. Our analysis leads to robust pairing mechanisms in  $d > 1$  of PDW order in a variety of continuum and lattice systems. Despite such robustness, we find that PDW order emerges from physically reasonable microscopic models only under special circumstances, which we precisely outline below. This perhaps accounts in part for why PDW order is so rare in real materials.

**Model and method of solution.**—We will study the fate of a Fermi liquid subject to a finite repulsive singlet BCS interaction:

$$H_{\text{pair}} = \sum_{ij} V_{ij} b_i^\dagger b_j, \quad b_i = c_{i\downarrow} c_{i\uparrow}. \quad (1)$$

In a translationally invariant system,  $V_{ij} = V(\mathbf{r}_i - \mathbf{r}_j)$ , and the interaction above can equivalently be expressed in momentum space as  $H_{\text{pair}} = \sum_{\mathbf{q}} V(\mathbf{q}) b_{\mathbf{q}}^\dagger b_{\mathbf{q}}$ .

We decouple the above interaction using an auxiliary field  $\phi$ , which corresponds to a charge  $2e$  pair field. The bare Euclidean Lagrangian density then consists of the metal, the pair fields, and a Yukawa coupling between them:  $\mathcal{L} = \mathcal{L}_f + \mathcal{L}_b + \mathcal{L}_g$ , where

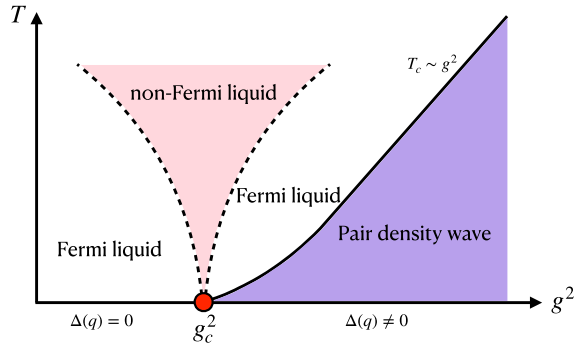


FIG. 1. Phase diagram obtained from the large- $N$  model. At  $T = 0$ , there is a QCP separating the PDW phase and the normal metallic state. The PDW transition temperature  $T_c$  scales linear in  $g^2$  in strong-coupling limit. Above the QCP, fluctuation of PDW gives rise to non-Fermi liquid behavior.

$$\begin{aligned}\mathcal{L}_f &= \sum_{\sigma=\uparrow,\downarrow} \int_y \psi_\sigma^\dagger(x) G_0^{-1}(x-y) \psi_\sigma(y), \\ \mathcal{L}_b &= \int_y \phi^\dagger(x) D_0^{-1}(x-y) \phi(y), \\ \mathcal{L}_g &= \eta g [\phi^\dagger(x) \psi_\uparrow(x) \psi_\downarrow(x) + \phi(x) \psi_\downarrow^\dagger(x) \psi_\uparrow^\dagger(x)].\end{aligned}\quad (2)$$

$x = (\mathbf{x}, \tau)$ ,  $\eta = 1(i)$  corresponds to attractive (repulsive) BCS couplings parametrized by a dimensionless coupling  $g$  (for the repulsive case, see Ref. [43] for details), and  $G_0$  and  $D_0$  are, respectively, the bare fermion and boson propagators in the decoupled limit  $g = 0$  (i.e.,  $D_0$  is proportional to the Fourier transform of the inverse  $[V(\mathbf{q})]^{-1}$ ).

The theory above can be solved for arbitrary  $g$  by considering a formal extension to large- $N$  limit where the fermion and boson fields are promoted to  $N$  component vectors that transform in the fundamental representation of a global  $SU(N)$  flavor symmetry group. The coupling between the fields is promoted to an all-to-all random Yukawa coupling in the space of flavors:

$$\begin{aligned}\mathcal{L}_g &\rightarrow \eta \sum_{km\ell} \left[ \frac{g_{km\ell}}{N} \psi_{k\uparrow}(x) \psi_{m\downarrow}(x) \phi_\ell^\dagger(x) \right. \\ &\quad \left. + \frac{g_{km\ell}^*}{N} \psi_{m\uparrow}^\dagger(x) \psi_{k\downarrow}^\dagger(x) \phi_\ell(x) \right],\end{aligned}\quad (3)$$

where the quenched random Yukawa couplings are spatially independent and are chosen from a Gaussian unitary ensemble with variance  $\overline{g_{km\ell} g_{k'm'\ell'}^*} = g^2 \delta_{kk'} \delta_{mm'} \delta_{\ell\ell'}$  and with zero average. The global  $SU(N)$  symmetry is thus only preserved on average. In terms of the original fermionic operators, this extension corresponds to the interaction of the form

$$H_{\text{pair}} = \sum_{ij} V_{ij} \sum_{\ell} b_{\ell i}^\dagger b_{\ell j}, \quad b_{\ell i} = \sum_{km} \frac{g_{km\ell}}{N} c_{ki\downarrow} c_{mi\uparrow}.\quad (4)$$

Using by now standard saddle point methods [44–48], the exact solution of the large- $N$  theory consists of self-consistent propagators  $G$ ,  $D$  with associated self-energies  $\Sigma$ ,  $\Pi$ :

$$\begin{aligned}\Sigma(k) &= -g^2 \sum_q \text{sgn}[V(\mathbf{q})] G(-k+q) D(q), \\ \Pi(q) &= -g^2 \text{sgn}[V(\mathbf{q})] \sum_k G(k) G(-k+q), \\ G(k) &= [G_0^{-1}(k) + \Sigma(k)]^{-1}, \quad D(q) = [D_0^{-1}(q) - \Pi(q)]^{-1}.\end{aligned}\quad (5)$$

Here,  $k = (\mathbf{k}, i\omega_n)$  and  $q = (\mathbf{q}, i\Omega_m)$ , where  $\omega_n (\Omega_m)$  are fermion (boson) Matsubara frequencies. The sign function  $\text{sgn}[V(\mathbf{q})]$  originates from the factor  $\eta$  introduced in Eq. (2). From the exact propagators  $G$ ,  $D$ , we extract all the salient physics, to obtain the schematic phase diagram in Fig. 1. For instance, to identify the finite temperature PDW transitions shown in Fig. 1, we need only consider the static bosonic propagator  $D(\mathbf{q})$ . The effective Ginzburg-Landau theory for the fields  $\phi$  will have a quadratic term whose coefficient is given by  $D^{-1}(\mathbf{q})$ . To study the manner in which the order parameter grows below the PDW transition, we again study the static bosonic propagators but now with the inclusion of nonlinear effects stemming from a nonzero vacuum expectation value of  $\phi$ . Finally, we will describe the PDW QCP and find the non-Fermi liquid behavior for the fermions.

*Fluctuating PDW order.*—We first show that when the interaction  $V(r)$  is *monotonic*, e.g.,  $V(r) \sim e^{-r/\xi}$ , the PDW order is absent for any  $g$ . The Fourier transform  $V(\mathbf{q})$  defines the bare inverse boson propagator, which is purely static, and takes an Ornstein-Zernike form:  $D_0^{-1}(\mathbf{q}) = r + c^2 q^2$ , with  $r > 0$ . To see why the theory fails to host long-range PDW order, consider the limit  $q/2k_F \ll 1$ , in which the saddle point solution for the exact static propagator  $D$  at  $T = 0$  can be analytically obtained:

$$D^{-1}(\mathbf{q}) = r + c^2 q^2 + g^2 \nu \log\left(\frac{4\omega_D}{v_F q}\right),\quad (6)$$

where the last term above is the contribution from the  $q \ll k_F$  limit of the static pair susceptibility,  $\omega_D$  is a cutoff, and  $\nu$  is the density of states at the Fermi level. Even at  $T = 0$ ,  $D^{-1}(\mathbf{q})$  remains positive, indicating the absence of a phase transition. Nevertheless, the minimum of  $D^{-1}(\mathbf{q})$  is at nonzero  $|\mathbf{q}| = \sqrt{(g^2 \nu / 2c^2)}$ , indicating softened pair fluctuations at finite momentum. Figure 2 shows  $D^{-1}(\mathbf{q})$  for various strengths  $g^2$ . With increasing  $g^2$ , the theory is driven further away from ordering, eventually having a correlation length short compared to the wavelength of the putative PDW—thus, a failed PDW. We next show that long-ranged PDW order occurs when the repulsive BCS couplings are nonmonotonic in space.

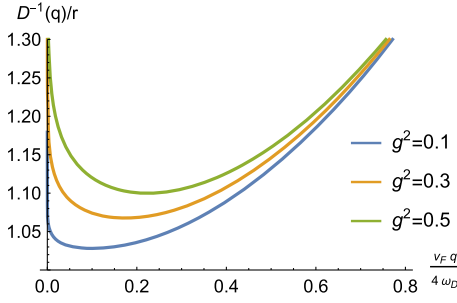


FIG. 2.  $D^{-1}(\mathbf{q})$  in the zero temperature limit obtained from Eq. (6). Here we set  $c^2/r = 0.5$ ,  $\nu/r = 0.1$ , and the momentum is measured in units of  $4\omega_D/v_F$ .

*PDWs from nonmonotonic BCS interactions.*—As an illustrative example, consider the case where the BCS coupling is nonzero only at a distance  $r_0$ :

$$V(\mathbf{r}) = g^2 \delta(\mathbf{r} - r_0), \quad V(\mathbf{q}) = 2\pi r_0 g^2 J_0(qr_0), \quad (7)$$

where  $J_0(x)$  is the zeroth Bessel function. Although  $V(\mathbf{r})$  is repulsive, its Fourier transform  $V(\mathbf{q})$  is an *oscillatory* function with both repulsive and attractive components [Fig. 3(a)]. The exact boson propagator in this case is

$$D^{-1}(\mathbf{q}) = \frac{1}{2\pi r_0 |J_0(qr_0)|} + g^2 \text{sgn}[V(\mathbf{q})] \Pi(\mathbf{q}). \quad (8)$$

To make sense of the above equation, we can approximate the boson self-energy  $\Pi(\mathbf{q})$  by the one-loop calculation  $\Pi_0(\mathbf{q})$  obtained using  $G_0$ . The result is shown in Fig. 3(b). Clearly we see that when  $V(\mathbf{q}) < 0$ , the associated Fourier components of  $D^{-1}(\mathbf{q})$  get smaller (i.e., closer to an ordering transition) as  $g^2$  increases whereas the repulsive components get larger. Nonetheless, the phase transition will not occur unless  $g^2$  exceeds a threshold value. In Fig. 3(c) we present the numerical results of  $D^{-1}(\mathbf{q})$  by solving the full saddle point equations (5) on a  $32 \times 32$  momentum mesh grid. The global minimum (dashed circle) of  $D^{-1}(\mathbf{q})$  indeed vanishes when  $T$  approaches  $T_c$ . Thus, there is a line of finite temperature phase transitions  $T_c(g^2)$  as  $g^2$  is varies, obtained by the condition  $D^{-1}(\mathbf{q}) = 0$ . For  $T > T_c$ , the minimum value of  $D^{-1}(\mathbf{q})$  forms a ring as is expected from the toy model, but stays positive. Once  $T$  approaches  $T_c$ , its minimum vanishes, indicating the PDW instability. Similarly, if we fix  $T$  instead and increase  $g^2$ , we can also see  $D^{-1}(\mathbf{q})$  vanishes at some finite  $g^2$ . In Fig. 3(d) we present  $T_c$  and a function of  $g^2$ . At large  $g^2$ , our result clearly shows a linear relation between  $T_c$  and  $g^2$ . The line of finite temperature transitions terminates at a  $T = 0$  phase transition at  $g = g_c$ .

Below the ordering transition, we must solve the self-consistent equations allowing for a nonzero expectation value  $\Delta(\mathbf{q}) = \langle \phi(\mathbf{q}) \rangle$ . Details of our calculation are provided

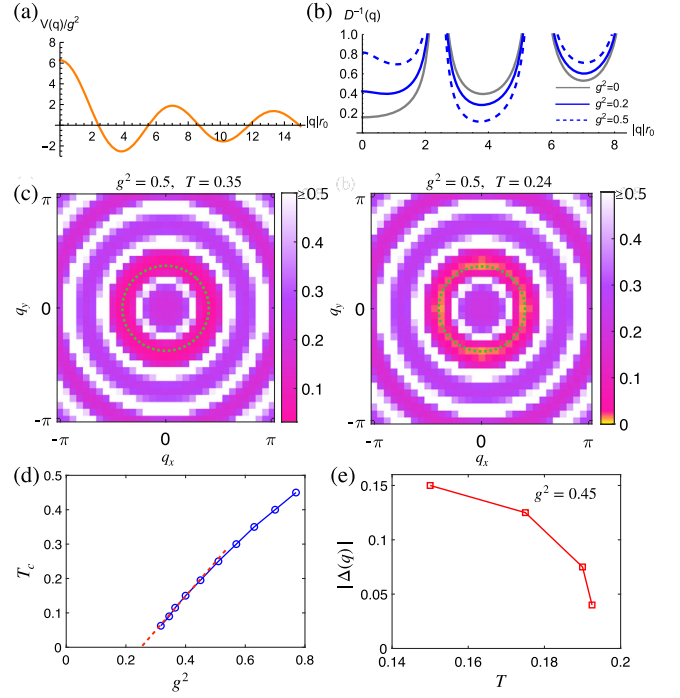


FIG. 3. (a)  $V(\mathbf{q})$  as a function of  $|\mathbf{q}|r_0$  with  $r_0 = 1$  from Eq. (7). (b)  $D^{-1}(\mathbf{q})$  at  $T = 0.05$  as a function of  $|\mathbf{q}|r_0$  (also with  $r_0 = 1$ ) obtained by approximating  $\Pi(\mathbf{q})$  in Eq. (8) by its one-loop calculation. (c) Density plot of  $D^{-1}(\mathbf{q})$  as a function of  $\mathbf{q}$  obtained by numerically solving the full saddle point equations in Eq. (5) with  $r_0 = 3$ . The two panels show the results for  $T$  above  $T_c$  and right at  $T_c$ , and the dashed circles mark the minimum of  $D^{-1}(\mathbf{q})$ . (d)  $T_c$  as a function of  $g^2$ . At large  $g^2$ , our result indicates that  $T_c$  scales linearly in  $g^2$ . (e) The magnitude of  $\Delta(\mathbf{q})$  below  $T_c$  for a given  $g^2 = 0.45$ . The energy scale here is measured in units of the Fermi energy  $E_F$ .

in Ref. [43]. Figure 3(e) shows  $\Delta(\mathbf{q})$  as a function of  $T$  below  $T_c$ . Within the accuracy of the numerical solutions, the expectation value grows continuously, indicating that the finite temperature transitions are second order and are well described by mean-field theory. From the solution of the nonlinear equations, we can also determine the ordering wave vector  $\mathbf{Q}$  of the PDW by minimizing  $D^{-1}(\mathbf{q})$  with respect to momentum:

$$\mathbf{Q}: \frac{d}{d\mathbf{q}} D^{-1}(\mathbf{q})|_{\mathbf{Q}} = 0. \quad (9)$$

In the neighborhood of  $\mathbf{Q}$ ,  $D^{-1}(\mathbf{q})$  takes the form  $D^{-1}(\mathbf{q}) = \gamma(|\mathbf{q}| - \mathbf{Q})^2$ , where  $\gamma = \frac{1}{2}(d^2/dq^2)D^{-1}(\mathbf{q})|_{\mathbf{Q}}$ .

*Lattice models with PDW order.*—Embodied by the simplified model above, we consider a more realistic example of electrons on a square lattice with nearest neighbor hopping  $t = 1$ , on-site Hubbard  $U$ , and second neighbor pair hopping  $J$ :

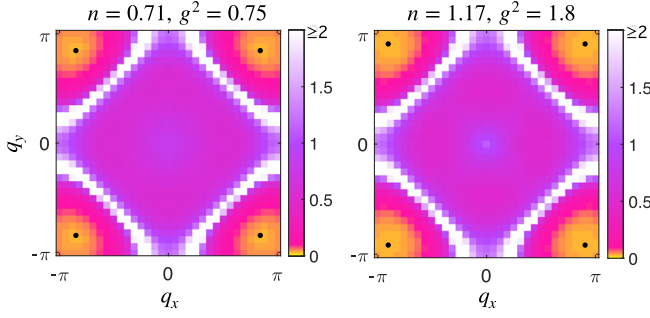


FIG. 4. Numerical solution of  $D^{-1}(\mathbf{q})$  from Eq. (10) obtained at a fixed  $T = 0.05$  with  $J = 2U$  for different fillings. In the left-hand panel there are  $n = 0.71$  electrons per site, and  $D^{-1}(\mathbf{q})$  touches zero at  $g^2 = 0.75$ . In the right-hand panel there are  $n = 1.17$  electrons per site, and  $g^2 = 1.8$  is the critical coupling where  $D^{-1}(\mathbf{q})$  touches zero. The black dots mark the positions of the ordering vector  $\mathbf{Q}$  near  $(\pm\pi, \pm\pi)$ , which leads to the PDW with checkerboard pattern in real space.

$$H = -t \sum_{\langle i,j \rangle, \sigma} c_{i\sigma}^\dagger c_{j\sigma} + U \sum_i n_{i\uparrow} n_{i\downarrow} + J \sum_{\langle i,j \rangle} c_{i\uparrow}^\dagger c_{i\downarrow}^\dagger c_{j\downarrow} c_{j\uparrow}, \quad (10)$$

where  $i, j$  above label lattice sites. The model above can similarly be  $N$  enhanced and the resulting saddle point solutions can be solved *mutatis mutandis*. In this case, the Fourier transform of the BCS interaction  $V(\mathbf{q})$  is  $V(\mathbf{q}) = U + 2J(\cos q_x + \cos q_y)$  and  $g^2 = U/t$ . As long as  $U < 4J$ ,  $V(\mathbf{q})$  can be negative at some finite  $\mathbf{q}$ . We solve Eq. (5) with the fermion dispersion replaced with  $\xi_{\mathbf{k}} = -2t(\cos k_x + \cos k_y) - \mu$ . The results are shown in Fig. 4. In this case, we have four symmetry-related ordering vectors at  $(\pm\pi, \pm\pi) + O(Ut/JE_F)$ , that depend on the strength of interactions and the filling. In this sense, the pairing state from the large- $N$  theory is different from the  $\eta$ -pairing state found in numerical studies of one-dimensional analogs of such models [31,49–52].

**PDW quantum critical point.**—Both the lattice and continuum models above have finite temperature continuous PDW transitions that terminate at the QCP. We can study the fate of itinerant fermions around this  $T = 0$  transition by solving the self-consistent set of equations in Eq. (5). A straightforward computation of the one-loop boson self-energy in the regime  $q \ll k_F$  yields (see Supplemental Material [43])  $\Pi(\mathbf{q}, i\Omega_m) = \nu[\ln(4\omega_D/v_F|\mathbf{q}|) - (|\Omega_m|/v_F|\mathbf{q}|)]$ . It then follows that in the limit  $q \ll k_F$ ,

$$D(q)^{-1} \approx \gamma(|\mathbf{q}| - Q)^2 + \frac{g^2 \nu |\Omega_m|}{v_F Q}, \quad (11)$$

resulting in a boson dynamical exponent  $z_b = 2$ . A fully self-consistent solution is obtained by computing the fermion self-energy using  $D(\mathbf{q})$  above. Performing the integrals in the  $z_b = 2$  scaling limit (see Supplemental

Material [43]), we obtain  $G^{-1}(\mathbf{k}, i\omega_n) = G_0^{-1}(\mathbf{k}) + \Sigma(\omega_n)$ , where

$$\Sigma(\omega_n) = i \text{sgn}(\omega_n) \omega_0^{1/2} |\omega_n|^{1/2}, \quad \omega_0 = \frac{g^2 Q}{\pi^2 v_F \gamma}. \quad (12)$$

The expressions for  $G, D$  are now fully self-consistent: upon feeding back the fermions to the boson,  $\Pi$  is unchanged. Thus, superconducting fluctuations are Landau overdamped and the fermions are dressed into a non-Fermi liquid. If, following Hertz [53], we were to integrate out the fermions, the bosonic sector would be at its upper critical dimension defined by  $d + z = 4$ , when  $d = 2$ . Thus, up to logarithmic corrections to scaling, the ordering transition has mean-field exponents, with  $\nu = 1/2$ . The line of finite temperature transitions emanates from the quantum critical point as  $T_c(g^2) \sim (g^2 - g_c^2)^{\nu z}$ , with unit exponent  $\nu z = 1$ . Note that in our toy model Eq. (7), the PDW ordering vector forms a ring, which renders the whole Fermi surface to be a “hot region” [54]. However, in the lattice model where there are only limited number of ordering vectors, there are only finite “hot spot” regions on the Fermi surface which has non-Fermi liquid behavior.

**Discussion.**—We have shown that PDW order arises unambiguously when electrons have sufficiently large repulsive and nonmonotonic BCS interactions. Interactions in the particle-hole channel can certainly destabilize the theory presented here. However, since ordering tendencies in the particle-hole channel require finite interaction strength, we expect our theory to remain robust, at least to the addition of weak interactions in the particle-hole channel [56]. Other possibilities include Kohn-Luttinger superconductivity, which also arises from repulsive interactions. However, such states are not present in the large- $N$  limit considered here, and are moreover at exponentially low temperature scales; by contrast, the PDW transitions occur at scales that exhibit power law dependence in the bare interactions of the system.

We speculate on the relevance of these results to real solids. In microscopic descriptions of solids, pair-hopping interactions are typically small compared to density-density interactions [57,58]. This is not true, however, in low energy effective descriptions, obtained from integrating out short-distance modes. We have concentrated on such pair-hopping terms in this Letter, since they give rise to site PDW orders, where each fermion of the Cooper pair “lives” on the same lattice site. Similar mechanisms can give rise to bond PDW order, where the pair is built from fermions separated by a nearest neighbor distance. In this case, the repulsive BCS interactions giving rise to PDW order are the more physically relevant density-density interactions, which are always sizable in any solid. Indeed, such density-density interactions can give rise to PDW order on the kagome lattice, as suggested in Ref. [59].

In addition, it is somewhat unusual to expect a relatively suppressed BCS repulsion at short distances. This requirement accounts at least in part for why PDW order is so seldom found in real materials. For the case of bond PDW order, Coulomb repulsion, in conjunction with strong coupling to Holstein phonons, can provide such nonmonotonic density-density interactions. This may account for recent studies of Hubbard-Holstein ladders reporting PDW order [60,61]. A promising system for realizing the conditions outlined here for PDW formation is electrons on a kagome lattice near the van Hove singularity. In this regime, the electrons have a peculiar property that short-distance Coulomb interactions are suppressed relative to nearest neighbor repulsion [62]. As a result, short-distance repulsive forces are suppressed relative to nearest neighbor repulsion, which is precisely the requisite condition for PDW order identified here. A recent study along these lines has shown that PDW order naturally arises at intermediate coupling on the kagome lattice [59]. We shall investigate the relevance of these findings to the phase diagram of kagome metals such as  $\text{CsV}_3\text{Sb}_5$  in future studies.

We thank D. Agterberg, A. Chubukov, R. Thomale, Z. Han, P. Hirschfeld, C. Murthy, S. Kivelson, and J. Sous for helpful discussions. S. R. and P. A. N. were supported by the Department of Energy, Office of Basic Energy Sciences, Division of Materials Sciences and Engineering, under Contract No. DE-AC02-76SF00515. Y.-M. W. acknowledges the Gordon and Betty Moore Foundation's EPIQS Initiative through GBMF8686 for support. A. A. P. is supported by the Flatiron Institute. The Flatiron Institute is a division of the Simons Foundation. We thank the participants of the ICTP 2022 workshop on Strongly Correlated Matter for enjoyable discussions.

- 
- [1] D. F. Agterberg, J. S. Davis, S. D. Edkins, E. Fradkin, D. J. Van Harlingen, S. A. Kivelson, P. A. Lee, L. Radzihovsky, J. M. Tranquada, and Y. Wang, The physics of pair-density waves: Cuprate superconductors and beyond, *Annu. Rev. Condens. Matter Phys.* **11**, 231 (2020).
- [2] P. Fulde and R. A. Ferrell, Superconductivity in a strong spin-exchange field, *Phys. Rev.* **135**, A550 (1964).
- [3] A. I. Larkin and Y. N. Ovchinnikov, Nonuniform state of superconductors, *Sov. Phys. JETP* **20**, 762 (1965).
- [4] C. C. Agosta, Inhomogeneous superconductivity in organic and related superconductors, *Crystals* **8**, 285 (2018).
- [5] Y. Matsuda and H. Shimahara, Fulde-Ferrell-Larkin-Ovchinnikov state in heavy fermion superconductors, *J. Phys. Soc. Jpn.* **76**, 051005 (2007).
- [6] A. Gurevich, Upper critical field and the Fulde-Ferrell-Larkin-Ovchinnikov transition in multiband superconductors, *Phys. Rev. B* **82**, 184504 (2010).
- [7] C.-w. Cho, J. H. Yang, N. F. Q. Yuan, J. Shen, T. Wolf, and R. Lortz, Thermodynamic Evidence for the Fulde-Ferrell-Larkin-Ovchinnikov State in the  $\text{KFe}_2\text{As}_2$  Superconductor, *Phys. Rev. Lett.* **119**, 217002 (2017).
- [8] E. Fradkin, S. A. Kivelson, and J. M. Tranquada, Colloquium: Theory of intertwined orders in high temperature superconductors, *Rev. Mod. Phys.* **87**, 457 (2015).
- [9] A. Himeda, T. Kato, and M. Ogata, Stripe States with Spatially Oscillating  $d$ -Wave Superconductivity in the Two-Dimensional  $t - t' - J$  Model, *Phys. Rev. Lett.* **88**, 117001 (2002).
- [10] K.-Y. Yang, W. Q. Chen, T. M. Rice, M. Sigrist, and F.-C. Zhang, Nature of stripes in the generalized  $t$ - $J$  model applied to the cuprate superconductors, *New J. Phys.* **11**, 055053 (2009).
- [11] M. Raczkowski, M. Capello, D. Poilblanc, R. Frésard, and A. M. Oleš, Unidirectional  $d$ -wave superconducting domains in the two-dimensional  $t - J$  model, *Phys. Rev. B* **76**, 140505(R) (2007).
- [12] E. Berg, E. Fradkin, E.-A. Kim, S. A. Kivelson, V. Oganesyan, J. M. Tranquada, and S. C. Zhang, Dynamical Layer Decoupling in a Stripe-Ordered High- $T_c$  Superconductor, *Phys. Rev. Lett.* **99**, 127003 (2007).
- [13] M. Capello, M. Raczkowski, and D. Poilblanc, Stability of RVB hole stripes in high-temperature superconductors, *Phys. Rev. B* **77**, 224502 (2008).
- [14] P. A. Lee, Amperean Pairing and the Pseudogap Phase of Cuprate Superconductors, *Phys. Rev. X* **4**, 031017 (2014).
- [15] Y. Wang, D. F. Agterberg, and A. Chubukov, Coexistence of Charge-Density-Wave and Pair-Density-Wave Orders in Underdoped Cuprates, *Phys. Rev. Lett.* **114**, 197001 (2015).
- [16] Y. Wang, D. F. Agterberg, and A. Chubukov, Interplay between pair- and charge-density-wave orders in underdoped cuprates, *Phys. Rev. B* **91**, 115103 (2015).
- [17] S. D. Edkins, A. Kostin, K. Fujita, A. P. Mackenzie, H. Eisaki, S. Uchida, S. Sachdev, M. J. Lawler, E.-A. Kim, J. C. S. Davis, and M. H. Hamidian, Magnetic field-induced pair density wave state in the cuprate vortex halo, *Science* **364**, 976 (2019).
- [18] Y. Wang, S. D. Edkins, M. H. Hamidian, J. C. Seamus Davis, E. Fradkin, and S. A. Kivelson, Pair density waves in superconducting vortex halos, *Phys. Rev. B* **97**, 174510 (2018).
- [19] G. B. Partridge, W. Li, R. I. Kamar, Y.-a. Liao, and R. G. Hulet, Pairing and phase separation in a polarized Fermi gas, *Science* **311**, 503 (2006).
- [20] M. W. Zwierlein, A. Schirotzek, C. H. Schunck, and W. Ketterle, Fermionic superfluidity with imbalanced spin populations, *Science* **311**, 492 (2006).
- [21] L. Radzihovsky and D. E. Sheehy, Imbalanced Feshbach-resonant Fermi gases, *Rep. Prog. Phys.* **73**, 076501 (2010).
- [22] H. Zhao, R. Blackwell, S. Ishida, H. Eisaki, A. Pasupathy, and K. Fujita (to be published).
- [23] Q. Gu, J. P. Carroll, S. Wang, S. Ran, C. Broyles, H. Siddiquee, N. P. Butch, S. R. Saha, J. Paglione, J. Davis *et al.*, Detection of a pair density wave state in  $\text{UTe}_2$ , [arXiv:2209.10859](https://arxiv.org/abs/2209.10859).
- [24] H. Chen, H. Yang, B. Hu, Z. Zhao, J. Yuan, Y. Xing, G. Qian, Z. Huang, G. Li, Y. Ye *et al.*, Roton pair density wave in a strong-coupling kagome superconductor, *Nature (London)* **599**, 222 (2021).
- [25] G. Y. Cho, J. H. Bardarson, Y.-M. Lu, and J. E. Moore, Superconductivity of doped Weyl semimetals: Finite-momentum pairing and electronic analog of the  $^3\text{He}$ - $a$  phase, *Phys. Rev. B* **86**, 214514 (2012).

- [26] G. Bednik, A. A. Zyuzin, and A. A. Burkov, Superconductivity in Weyl metals, *Phys. Rev. B* **92**, 035153 (2015).
- [27] Y. Wang and P. Ye, Topological density-wave states in a particle-hole symmetric Weyl metal, *Phys. Rev. B* **94**, 075115 (2016).
- [28] Y. Li and F. D. M. Haldane, Topological Nodal Cooper Pairing in Doped Weyl Metals, *Phys. Rev. Lett.* **120**, 067003 (2018).
- [29] Y.-M. Wu, Z. Wu, and H. Yao, Pair-density-wave and chiral superconductivity in twisted bilayer transition-metal-dichalcogenides, [arXiv:2203.05480](https://arxiv.org/abs/2203.05480).
- [30] Z. Wu, Y.-M. Wu, and F. Wu, Pair density wave and loop current promoted by van Hove singularities in moiré systems, [arXiv:2207.11468](https://arxiv.org/abs/2207.11468).
- [31] B. Bhattacharyya and G. K. Roy, The ground state of the Penon-Kolb-Hubbard model, *J. Phys. Condens. Matter* **7**, 5537 (1995).
- [32] J. Wårdh and M. Granath, Effective model for a supercurrent in a pair-density wave, *Phys. Rev. B* **96**, 224503 (2017).
- [33] J. Wårdh, B. M. Andersen, and M. Granath, Suppression of superfluid stiffness near a Lifshitz-point instability to finite-momentum superconductivity, *Phys. Rev. B* **98**, 224501 (2018).
- [34] E. Berg, E. Fradkin, and S. A. Kivelson, Pair-Density-Wave Correlations in the Kondo-Heisenberg Model, *Phys. Rev. Lett.* **105**, 146403 (2010).
- [35] F. Loder, A. P. Kampf, and T. Kopp, Superconducting state with a finite-momentum pairing mechanism in zero external magnetic field, *Phys. Rev. B* **81**, 020511(R) (2010).
- [36] F. Loder, S. Graser, A. P. Kampf, and T. Kopp, Mean-Field Pairing Theory for the Charge-Stripe Phase of High-Temperature Cuprate Superconductors, *Phys. Rev. Lett.* **107**, 187001 (2011).
- [37] C. Setty, L. Fanfarillo, and P. J. Hirschfeld, Microscopic mechanism for fluctuating pair density wave, [arXiv:2110.13138](https://arxiv.org/abs/2110.13138).
- [38] C. Setty, J. Zhao, L. Fanfarillo, E. W. Huang, P. J. Hirschfeld, P. W. Phillips, and K. Yang, Exact solution for finite center-of-mass momentum cooper pairing, [arXiv:2209.10568](https://arxiv.org/abs/2209.10568).
- [39] H.-C. Jiang, Pair density wave in doped three-band Hubbard model on square lattice, [arXiv:2209.11381](https://arxiv.org/abs/2209.11381).
- [40] J.-T. Jin, K. Jiang, H. Yao, and Y. Zhou, Interplay between Pair Density Wave and a Nested Fermi Surface, *Phys. Rev. Lett.* **129**, 167001 (2022).
- [41] Z. Han and S. A. Kivelson, Pair density wave and reentrant superconducting tendencies originating from valley polarization, *Phys. Rev. B* **105**, L100509 (2022).
- [42] Y. Yu, V. Madhavan, and S. Raghu, Majorana fermion arcs and the local density of states of  $\text{UTe}_2$ , *Phys. Rev. B* **105**, 174520 (2022).
- [43] See Supplemental Material at <http://link.aps.org/supplemental/10.1103/PhysRevLett.130.026001> for details about decoupling the BCS repulsion, as well as calculating the pair susceptibility, nonlinear gap equation and fermion self energy.
- [44] I. Esterlis and J. Schmalian, Cooper pairing of incoherent electrons: An electron-phonon version of the Sachdev-Ye-Kitaev model, *Phys. Rev. B* **100**, 115132 (2019).
- [45] I. Esterlis, H. Guo, A. A. Patel, and S. Sachdev, Large- $N$  theory of critical Fermi surfaces, *Phys. Rev. B* **103**, 235129 (2021).
- [46] E. E. Aldape, T. Cookmeyer, A. A. Patel, and E. Altman, Solvable theory of a strange metal at the breakdown of a heavy Fermi liquid, *Phys. Rev. B* **105**, 235111 (2022).
- [47] A. A. Patel and S. Sachdev, Critical strange metal from fluctuating gauge fields in a solvable random model, *Phys. Rev. B* **98**, 125134 (2018).
- [48] Y. Wang, Solvable Strong-Coupling Quantum-Dot Model with a Non-Fermi-Liquid Pairing Transition, *Phys. Rev. Lett.* **124**, 017002 (2020).
- [49] C. N. Yang,  $\eta$  Pairing and Off-Diagonal Long-Range Order in a Hubbard Model, *Phys. Rev. Lett.* **63**, 2144 (1989).
- [50] C. N. Yang and S. Zhang,  $\text{So}_4$  symmetry in a Hubbard model, *Mod. Phys. Lett. B* **04**, 759 (1990).
- [51] A. Hui and S. Doniach, Penon-Kolb-Hubbard model: A study of the competition between single-particle and pair hopping in one dimension, *Phys. Rev. B* **48**, 2063 (1993).
- [52] G. I. Japaridze and E. Müller-Hartmann, Bond-located ordering in the one-dimensional Penon-Kolb-Hubbard model, *J. Phys. Condens. Matter* **9**, 10509 (1997).
- [53] J. A. Hertz, Quantum critical phenomena, *Phys. Rev. B* **14**, 1165 (1976).
- [54] Despite this peculiarity, fluctuation-induced first order transitions along the lines of Ref. [55] are absent in the large- $N$  limit since all dynamically generated nonlinear terms in the boson effective potential are  $1/N$  suppressed. Nevertheless, at finite  $N$ , we can argue against such first order transitions if we view the toy model in the continuum limit as applying to a dilute electron system on a lattice. In this case, corrections to effective mass will lift the degeneracy and reduce the hot regions on the Fermi surface to hot spots.
- [55] S. A. Brazovskii, Phase transition of an isotropic system to a nonuniform state, *Sov. J. Exp. Theor. Phys.* **41**, 85 (1975).
- [56] H.-C. Jiang, Y.-M. Wu, and S. Raghu (to be published).
- [57] S. Kivelson, W.-P. Su, J. R. Schrieffer, and A. J. Heeger, Missing Bond-Charge Repulsion in the Extended Hubbard Model: Effects in Polyacetylene, *Phys. Rev. Lett.* **58**, 1899 (1987).
- [58] J. Hirsch, Bond-charge repulsion and hole superconductivity, *Physica (Amsterdam)* **158C**, 326 (1989).
- [59] Y.-M. Wu, R. Thomale, and S. Raghu, Sublattice interference promotes pair density wave order in kagome metals, [arXiv:2211.01388](https://arxiv.org/abs/2211.01388).
- [60] K. S. Huang, Z. Han, S. A. Kivelson, and H. Yao, Pair-density-wave in the strong coupling limit of the Holstein-Hubbard model, *npj Quantum Mater.* **7**, 1 (2022).
- [61] Z. Han, S. A. Kivelson, and H. Yao, Strong Coupling Limit of the Holstein-Hubbard Model, *Phys. Rev. Lett.* **125**, 167001 (2020).
- [62] M. L. Kiesel and R. Thomale, Sublattice interference in the kagome Hubbard model, *Phys. Rev. B* **86**, 121105(R) (2012).